

# Multifractal Analysis of Geochemical Stream Sediment Data in Bange Region, Northern Tibet

Xianzhong Ke<sup>1,2</sup>, Shuyun Xie<sup>\*3,4</sup>, Youye Zheng<sup>3</sup>, Salah Fadlallah Awadelseid<sup>4</sup>,  
Shunbao Gao<sup>2</sup>, Liming Tian<sup>2</sup>

1. Geological Survey of China University of Geosciences, Wuhan 430074, China

2. Faculty of Earth Resources, China University of Geosciences, Wuhan 430074, China

3. State Key Laboratory of Geological Processes and Mineral Resources, China University of Geosciences, Wuhan 430074, China

4. School of Earth Sciences, China University of Geosciences, Wuhan 430074, China

**ABSTRACT:** The aim of this study is to quantify the geochemical elements distribution patterns analyzed from stream sediment data and then to delineate favorable areas for mineral exploration. A total of 7 270 stream sediment samples were collected from four subareas and 37 rock (ore) chip samples from five different locations in the Bange region, northern Tibet (China). The multifractal spectra of 12 elements including Au, Ag, As, Cu, Mo, Pb, Zn, W, Sn, Bi, Sb and Hg are represented by the method of moments, and characterized by five quantitative multifractal parameters. The results show that the multifractality for Cu and Bi in the Gongma area is much stronger than those in other subareas. Both the asymmetry index of multifractal spectra and the variance coefficients of Cu and Bi in this area are the highest, which imply that the distribution pattern of Cu and Bi in the Gongma area is the most heterogeneous. These multifractal parameters indicate that the Gongma area is the most favorable for prospecting Cu and Bi. The results obtained by the method of moments are in agreement with petrochemical analysis and field observation. It is suggested that multifractal analysis can be used as an effective tool to evaluate the ore-forming potential in the study area and to provide new approaches for geochemical exploration.

**KEY WORDS:** stream sediment, the method of moments, multifractal spectrum, ore-forming potential, Tibet.

## 0 INTRODUCTION

To identify the distribution patterns of geochemical elements and to delineate target areas for mineral exploration are essential objectives of exploration geochemistry. Exploration geologists often need to separate anomalies associated with mineralization from background reflecting regional geological processes. Various quantitative methods have been developed to model the distribution patterns of geochemical elements, and among them, the conventional and spatial statistical methods have played important roles (Cheng et al., 1996; Sinclair, 1991; Stanley and Sinclair, 1989; Grunsky and Agterberg, 1988; Stanley, 1988). In addition to frequency distributions and spatial correlation and variability of concentration values, geometrical properties and scale-independent characteristics of anomalies can be considered in fractal/multifractal methods (Cheng et al., 1997, 1996, 1994).

The developments of fractal and multifractal theory in the

past 30 years have shown that many geological processes (including mineralization, sedimentation, volcanism, igneous activity and geomorphology) exhibit self-similarity or self-affinity, which can result in fractals and multifractals with scale-independent characteristics (Cheng, 1999a). The application of fractal/multifractal offered a new horizon to the understanding of irregularities of geological features and the spatial distribution patterns of geological objects (Carranza, 2009; Raines, 2008; Wang et al., 2008, 2006; Cheng and Agterberg, 1996, 1995; Cheng, 1995; Mandelbrot, 1983) and the properties of mineralization (Gumiel et al., 2010; Turcotte, 2002, 1997; Shi and Wang, 1998; Li et al., 1994; Sanderson et al., 1994; Carlson, 1991). Fractal and multifractal techniques have been extensively used to characterize spatial structures of geochemical data for mineral exploration (Zuo, 2011; Zuo et al., 2009; Xie et al., 2008, 2007; Xie and Bao, 2004a, b, 2003a, b; Cheng, 1999a; Cheng et al., 1996, 1994; Xie and Yin, 1993).

The Gangdese metallogenic belt is one of the most important areas for mineral exploration in China, where large amount of mineral deposits (e.g., Qulong, Jiama, Chongjiang, Tinggong, Zhunuo, etc.) have been discovered in recent years (Li et al., 2004). In the past two decades, several geological surveys and resource assessments have been carried out in this belt by the China Geological Survey, showing that it is prospective for

\*Corresponding author: tinaxie2006@gmail.com

© China University of Geosciences and Springer-Verlag Berlin Heidelberg 2015

Manuscript received January 7, 2015.

Manuscript accepted April 10, 2015.

copper polymetallic deposits in the belt (Rui et al., 2006, 2003; Wang et al., 2002; Zheng et al., 2002; Qu et al., 2001). Most researches in this belt have focused on geology, geochemistry, evolution history, mineral exploration and genesis of porphyry copper deposits (Hou et al., 2009; Li et al., 2009; She et al., 2009; Pan et al., 2006; Zheng et al., 2003). Recently, fractal/multifractal models have been applied in this belt for mineral exploration (Zuo, 2011; Xie et al., 2010, 2008; Zuo et al., 2009).

In this paper, a total of 7 270 stream sediment samples were collected from four different subareas (Duoba, Gongma, Jiurucuo and Bange County) at a mapping scale of 1 : 50 000 and 37 rock (ore) chips were sampled in five different localities (Biangari (BGR), Duoria (DRA), Longga (LG), Quru (QR) and Gangguo (GG)) in the Bange region, northern Tibet (China). The stream sediment samples were analyzed for 12 elements (Au, Ag, As, Cu, Mo, Pb, Zn, W, Sn, Bi, Sb, and Hg) and processed by the method of moments in order to evaluate the ore-forming potential of copper and bismuth in these areas. The petrochemical analysis and the field observation were used to verify and check the results obtained by the method of moments.

## 1 GEOLOGICAL SETTING AND GEOCHEMICAL DATA

### 1.1 Regional Geological Background and Ore Deposit Geology

The study area, the Bange region, is located north of Tibet. It belongs to the Bange-Tengchong volcanic-magmatic arc belt in the northern Gangdese block, and is located in the southern part of the central Bangonghu-Nujiang suture zone (Fig. 1b, grey polygon). It was demonstrated that the formation of the Bange-Tengchong volcanic-magmatic arc belt was mainly the result of the southward subduction of the Bangonghu-Nujiang Ocean (Gao et al., 2011a; Zhu et al., 2006). The host rocks in this belt consist of Late Paleozoic to Cenozoic sedimentary rocks (conglomerate, sandstone and carbonate). The Paleozoic sedimentary rocks are mainly distributed in the Shenzha County and the Luolong-Basu region. The Mesozoic and Cenozoic sedimentary rocks are widely distributed in this belt, which are represented by Jurassic and Cretaceous formations. The magmatic rocks in this belt comprise Late Carboniferous and Jurassic to Cretaceous rocks. The Cretaceous magmatic rock is the most widely distributed (Gao et al., 2011b). The faults in this belt mainly have NW trend, and some faults have NE and E-W trends. The magmatic intrusions in this belt were structurally controlled by these fault systems. The NW-trending faults controlled the distribution of the Early Cretaceous granite, while the NE-trending faults controlled the distribution of the Late Yanshanian granite (Zhang et al., 2011).

The Bange-Tengchong volcanic-magmatic arc belt is considered to be a polymetallic belt where Fe, Cu, Pb, Zn, W, Sn, Au, Hg, Sb, Cr, and REE deposits occur (Gao et al., 2011b; Zhang et al., 2011; Rui et al., 2006). The Pb and Zn deposits, which are mainly distributed in the eastern part of this belt (e.g., Basu, Ranwu and Boshulaling), include hydrothermal veins, carbonate-and/or clastic-hosted and skarn types. The dominant

ore deposits in the central part of this belt (Bange region) are Cu-Fe polymetallic deposits of skarn type, W and Sn deposits of greisen type and placer Sn and Au deposits. The Hg, Sb, Cr, and REE occur as small deposits in some places in northern Tibet (Rui et al., 2006).

In the study area, sedimentary rocks, such as the NW-trending Lower Cretaceous Langshan Formation, are widely distributed in the central part of the Gongma area and the southern part of the Jiurucuo area (Fig. 1a). The dominant rocks in these areas are terrigenous clastic rocks and carbonate rocks, which are represented by the Yongzhu and Langshan formations, respectively. The Cu-Fe mineralization is related to the Langshan Formation in the Gongma area.

Outcrops of volcanic rocks are rare in the study area, and such rocks occurring only as interlayers distributed discretely in the central-upper Jurassic Lagongtang Formation in the eastern part of the Bange County area (Gao et al., 2011b). However, Yanshanian intrusive rocks are mainly composed of two major geological units (monzogranites and granodiorites) and are extensively distributed in the central and northern parts of the study area, accounting for approximately 50 percent of the total area (Fig. 1a) (Gao et al., 2011b).

The greatest achievement in the latest exploration in this area was the discovery of the Ria Cu-Fe polymetallic deposit (Fig. 1a), which is composed of three ore blocks and eight orebodies with different sizes (50–300 m in length) (Gao et al., 2011b). The chemical compositions of the orebodies are characterized by average contents of 1.07% Cu, 3.24% Pb, 1.93% Zn, and 0.015% Ag.

### 1.2 Geochemical Data

With an average density of four samples per square kilometer, a total of 7 270 stream sediments samples were collected from four subareas measuring a total area of 1 748 km<sup>2</sup>: 1 789 samples from the Duoba area, 2 328 samples from the Gongma area, 1 711 samples from the Jiurucuo area and 1 442 samples from the Bange County area. These samples were analyzed for 12 major ore-forming elements (Au, Ag, As, Cu, Mo, Pb, Zn, W, Sn, Bi, Sb, and Hg) by the Mineral Resources Analyzing Centre of Ministry of Land and Resource, Shenyang. The concentrations of Au were determined by graphite furnace-atomic absorption spectrometry (GF-AAS). Ag and Sn by atomic emission spectrometry (AES). Cu, Pb and Zn by inductively coupled plasma optical emission spectrometer (ICP-OES). As, Sb, Bi and Hg by atomic fluorescence spectrometry (AFS) and W and Mo by inductively coupled plasma-mass spectrometry (ICP-MS). The method detection limits for Au, Ag, Sn, Cu, Pb, Zn, As, Sb, Bi, Hg, W, and Mo were 0.000 3, 0.02, 1, 1, 2, 4, 0.6, 0.05, 0.05, 0.000 5, 0.04, and 0.04 µg/g, respectively.

Thirty-seven rock (ore) chips were sampled (Fig. 1a) and the contents of Cu, Pb, Zn, and Ag were analyzed by the Mineral Resources Analyzing Centre of Ministry of Land and Resource, Wuhan. The contents of Cu, Pb, Zn and Ag were measured by flame atomic absorption spectroscopy (AAS), whereby the average analytical error was less than 5% and the reproducibility of duplicate analyses was generally within 10%.

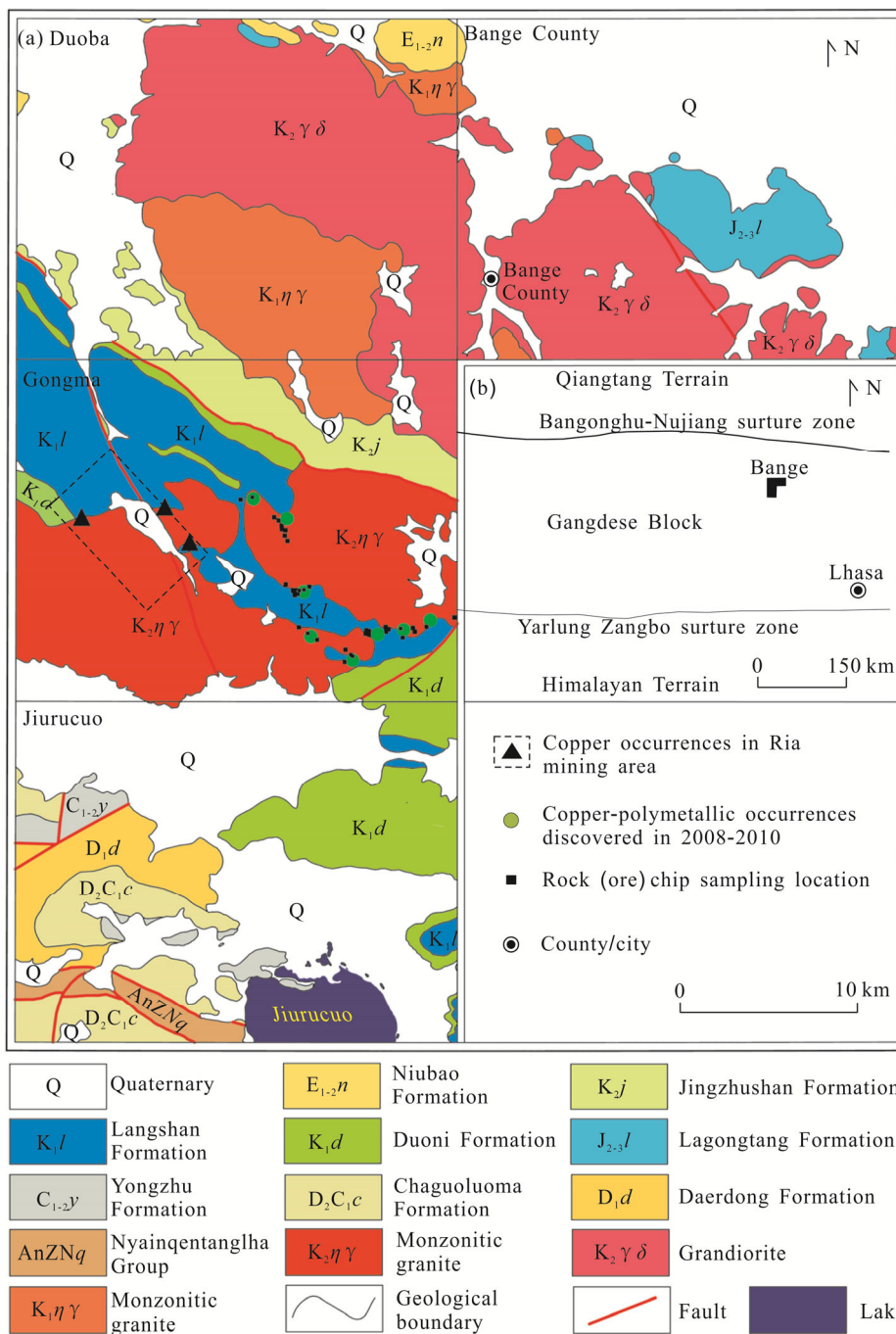


Figure 1. Geological map and rock (ore) chip samples location in the Bange region, Tibet ((b) is revised from Gao et al., 2011a).

The statistical properties of the geochemical data for the stream sediment samples are summarized in Table 1. The differences between the means of elements in the different areas are very clear (e.g., the means of Cu, Mo, Pb, and Bi in the Gongma area are much higher than those in the other three subareas). The coefficients of variation of the individual elements are also variable in the different subareas (e.g., the coefficients of variation of Cu and Bi in the Gongma area are much higher than those in the other three subareas), indicating distinct distribution patterns of geochemical concentrations in the different subareas (Table 1).

## 2 THE METHOD OF MOMENTS

It has been demonstrated that element concentrations in geochemical fields exhibit fractal or multifractal characteristics. Many methods have been proposed to study and describe the multifractal characteristics of element concentrations, among which the method of moments is commonly used (Xie et al., 2010, 2008, 2007; Xie and Bao, 2004a, b, 2003a, b; Xie, 2003; Agterberg, 2001; Cheng, 1999b; Evertsz and Mandelbrot, 1992; Halsey et al., 1986). In order to perform a multifractal analysis, a measure related to local concentrations should be defined in sampling space. Firstly, a measure  $\mu_i(\epsilon)$  for a box  $i$  in the sampling space can be defined as

$$\mu_i(\varepsilon) = x_i \varepsilon^2 \quad (1)$$

where  $x_i$  is the average concentration of an element in the sampling space with  $\varepsilon$  box size (Cheng, 1999b). The partition function,

$$x_q(\varepsilon) = \sum_{i=1}^{n(\varepsilon)} \mu_i^q \quad (2)$$

results from a weighted sum over all boxes, where  $n(\varepsilon)$  is the number of boxes covering the sampling space, and  $q$  is the moment of the weighted sum (Halsey et al., 1986). If the distribution pattern of  $x_q(\varepsilon)$  is multifractal, then the relationship

between  $x_q(\varepsilon)$  and box size  $\varepsilon$  can be described as below

$$x_q(\varepsilon) \propto \varepsilon^{\tau(q)} \quad (3)$$

where  $\tau(q)$  is the mass exponent (Feder, 1988), which is a function of  $q$ . Monofractal sets display a linear  $\tau(q)$  spectrum with  $\tau(q) = \alpha q - 1$ , where  $\alpha$  is the global Hölder exponent, which is a singularity index of geochemical data. For multifractal measures,  $\tau(q)$  is the nonlinear function  $\tau(q) = \alpha q - f(\alpha)$ , where  $\alpha = d\tau/dq$  is not constant and  $f(\alpha)$  is the fractal dimension.

**Table 1** Statistical properties of geochemical data for elements analyzed in stream sediment samples from the Bange region, Tibet. Data are in ppm, except for Au (ppb). Cv. Coefficient of variation

| Elements | Duoba |      | Gongma |       | Jiurucuo |      | Bange County |      |
|----------|-------|------|--------|-------|----------|------|--------------|------|
|          | Mean  | Cv   | Mean   | Cv    | Mean     | Cv   | Mean         | Cv   |
| Au       | 1.02  | 1.63 | 0.98   | 0.63  | 0.91     | 1.95 | 0.76         | 4.71 |
| Ag       | 0.076 | 0.43 | 0.119  | 3.50  | 0.074    | 0.24 | 0.074        | 0.32 |
| As       | 17.70 | 0.73 | 15.10  | 0.61  | 15.91    | 0.40 | 16.21        | 0.62 |
| Cu       | 13.55 | 0.50 | 27.04  | 10.04 | 14.79    | 0.39 | 12.38        | 0.38 |
| Mo       | 0.53  | 0.37 | 0.82   | 1.58  | 0.55     | 0.46 | 0.46         | 0.38 |
| Pb       | 27.46 | 0.52 | 44.58  | 1.72  | 30.31    | 0.25 | 28.21        | 0.20 |
| Zn       | 48.41 | 0.37 | 67.45  | 1.30  | 58.18    | 0.42 | 46.72        | 0.34 |
| W        | 4.61  | 0.99 | 5.92   | 1.89  | 2.54     | 0.38 | 4.14         | 1.53 |
| Sn       | 5.48  | 1.89 | 5.09   | 1.83  | 2.72     | 0.31 | 5.29         | 1.67 |
| Bi       | 0.49  | 0.81 | 2.99   | 15.48 | 0.49     | 0.67 | 0.44         | 0.74 |
| Sb       | 1.01  | 0.56 | 1.02   | 0.64  | 1.10     | 0.38 | 0.88         | 0.42 |
| Hg       | 0.018 | 0.68 | 0.017  | 0.51  | 0.02     | 0.59 | 0.019        | 1.16 |

To calculate the multifractal parameters,  $q$  was selected in the range from -10 to 10 with an interval of 0.5 to construct the partition functions  $x_q(\varepsilon)$ . With standard errors less than 0.05 and correlation coefficient  $|r| > 0.97$ , the slopes of straight lines of  $\log(x_q(\varepsilon)) - \log(\varepsilon)$ ,  $\tau(q)$ , are estimated using a least squares fit. The singularity exponent  $\alpha(q)$  and the multifractal spectrum  $f(\alpha)$  can then be obtained. Multifractality, represented by  $\tau''(1)$  ( $\tau(2) - 2\tau(1) + \tau(0)$ ), is calculated and proved to be associated with spatial analysis parameters (Cheng, 1999b). The widths of the singularity spectrum  $f(\alpha)$ , i.e.,  $\Delta\alpha = \alpha_{q_{\min}} - \alpha_{q_{\max}}$ , are also calculated. To characterize the shapes of the multifractal spectrum, the asymmetry index,  $R = (\Delta\alpha_L - \Delta\alpha_R) / (\Delta\alpha_L + \Delta\alpha_R)$ , is also calculated, where  $\Delta\alpha_R (\alpha_{q_{\min}} - \alpha_0)$  is the width of the right branch of the multifractal spectrum curve and  $\Delta\alpha_L (\alpha_0 - \alpha_{q_{\max}})$  is the width of the left branch of the multifractal spectrum curve (Xie and Bao, 2004a).

### 3 RESULTS AND DISCUSSION

#### 3.1 Multifractal Distribution Patterns of Ore-Forming Elements

The multifractal spectrum curves ( $f(\alpha)$ ) of the 12 studied elements, calculated by the method of moments (Fig. 2), are all continuous and asymmetric with convex shape. This indicates that the distribution patterns of individual elements in the geochemical fields of the studied region are multifractal and all the

geochemical fields of the 12 studied elements have experienced different degrees of superposition (Xie and Bao, 2004a). The maximum of a multifractal curve is attained by one value of  $\alpha$ , called  $\alpha_0$ , and around this maximum there are two branches of the curve: one is the left branch with all singularity values  $\alpha$  smaller than  $\alpha_0$  and the other is the right branch with  $\alpha$  greater than  $\alpha_0$ . For all the element concentration values, the multifractal spectrum curves are not symmetrical around the maximum, some deviating to the left part and some to right (Xie, 2003). For the left-deviating continuous multifractal spectrum curves, the right branches are shorter than the left branches, showing that higher concentration values are much enriched. For the right-deviating continuous multifractal spectrum curves, the right branches reflect depletion of element concentrations (Xie and Bao, 2004a). The multifractal spectrum curves of the different elements or the same elements are different in the individual subareas. Taking Cu in the four subareas as an example, the multifractal spectrum curves for Cu in the Gongma and Bange County areas are left-deviating but those in the Duoba and Jiurucuo areas are right-deviating.

The  $\Delta\alpha$  value, the width of the multifractal spectrum curve, reflects the enrichment of concentration of elements in a local space. A high  $\Delta\alpha$  value means that the concentrations of an element are more variable and enriched, indicating a complicated distribution pattern in a geochemical field, which is fa-

favorable for ore-formation. The  $\Delta\alpha_L$  and  $\Delta\alpha_R$  are the widths of the left and right branches, respectively, in a multifractal spectrum curve. The  $\Delta\alpha_L$  value mainly describes the distribution pattern of high element contents in a geochemical field. The higher the  $\Delta\alpha_L$  value, the stronger the singularity is, implying favorability for ore-formation. The  $\Delta\alpha_R$  value reflects the distribution pattern of low element contents (Xie and Bao, 2004b, 2003a, b; Agterberg, 2001; Cheng, 2000a; Evertsz and Man-

delbrot, 1992). The asymmetry index ( $R$ ) is used to quantitatively describe the deviation of an asymmetric multifractal spectrum curve to a symmetric one. The higher the  $R$  value, the wider the left branch of the curve is and the stronger the singularity of element concentrations, providing useful information for ore-forming potential assessment of elements (Xie and Bao, 2004a, b, 2003a, b; Xie, 2003).

The  $\Delta\alpha$ ,  $\Delta\alpha_L$  and  $R$  values for the main ore-forming ele-

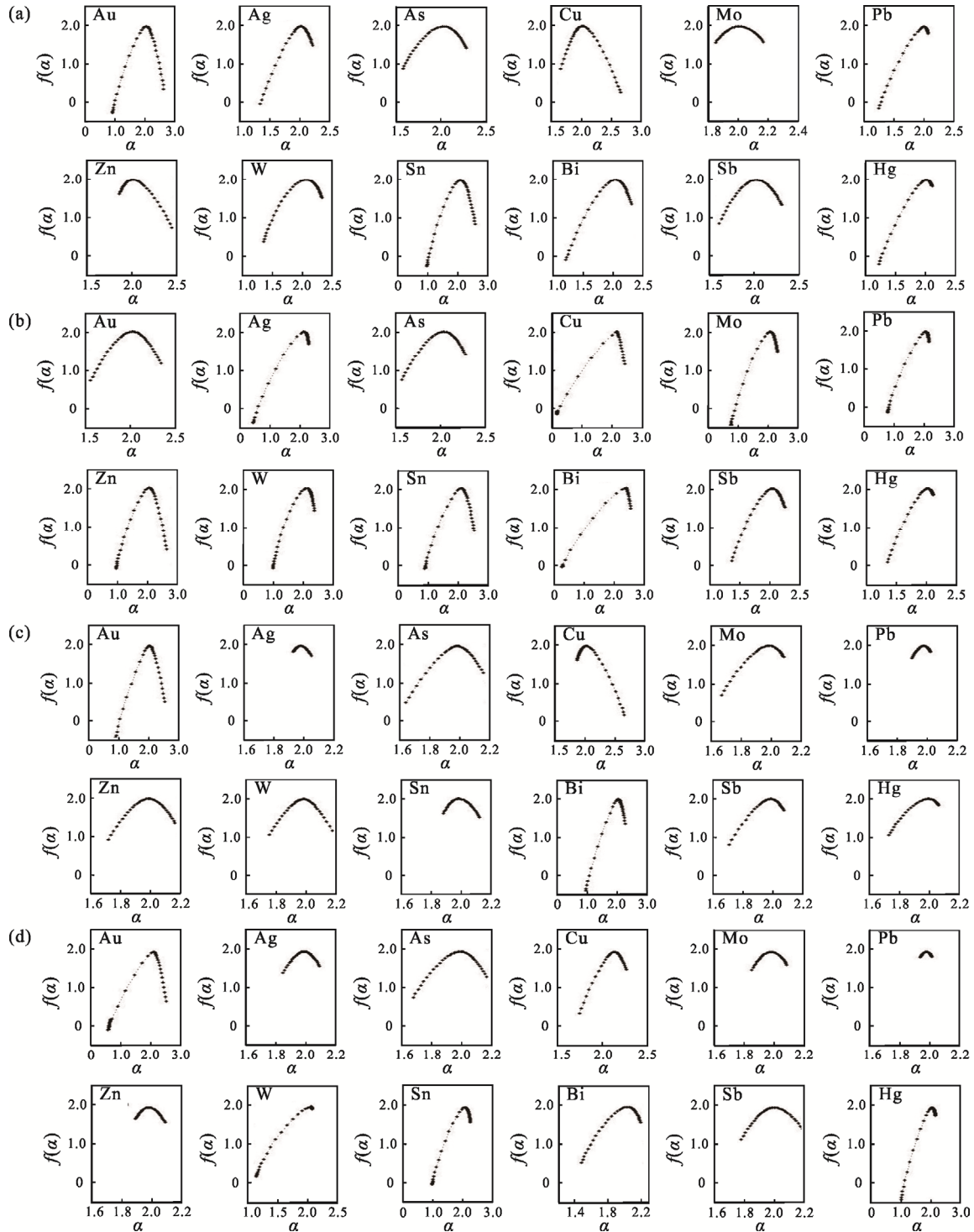


**Figure 2.** Multifractal spectrum curves of 12 elements in stream sediment samples from the Bange region, Tibet. (a) Duoba area; (b) Gongma area; (c) Jiurucuo area; (d) Bange County area.

ments Cu, Pb, Zn, Ag, Mo, Bi, W, and Sn in the Gongma area are notably greater than those in the other three subareas. The corresponding  $\tau''(1)$  values ( $\tau(2)-2\tau(1)+\tau(0)$ ) of the eight main ore-forming elements in the Gongma area are lower than those in the other subareas. The  $\Delta\alpha_R$  values of Ag, Cu, W, and Sn in the Jiurucuo area, are higher than or close to the corresponding  $\Delta\alpha_L$  value, resulting in lower  $R$  values in that area (Table 2).

The geochemical maps for Au, Ag, As, Cu, Pb, Zn, W, Sn, Mo, Bi, Sb, and Hg, which are derived by means of an inverse distance weighted moving average method were created by GeoDAS software (Cheng, 2000b), are shown in Fig. 3. The moving averaging used a square window of size  $0.4 \times 0.4 \text{ km}^2$ , distance decay exponent 2 and minimum number of samples equal to 16. It is shown that the main ore-forming elements Cu, Pb, Zn, Ag, Mo, Bi, W, and Sn are enriched in the Gongma area apparently and are spread in the NW-trending, and these distribution of the main ore-forming elements are controlled by that of the geological background. It can be inferred that the elements distribution may be related to the skarn type mineralization in the Gongma area. On the contrary, the elements Ag,

Cu, W, and Sn in the Jiurucuo area are not concentrated with low content distribution. The distribution of elements in the geochemical maps is in accordance with the parameters calculated by the method of moments.

The multifractal parameters  $\Delta\alpha$  and  $\Delta\alpha_L$  for Cu and Bi in the Gongma area are 2.231, 2.251 and 1.943, 2.035, respectively, which are much higher than those in the other three subareas, indicating that the concentrations of the two elements in the Gongma area are more heterogeneous. The asymmetry index  $R$  for Cu (0.762) and Bi (0.814) in the Gongma area are the maximum, which implies the strongest singularity of the two elements in the four subareas. The greatest coefficient of variation values (Table 1) also show the dispersed and locally enriched distribution patterns of Cu and Bi in the Gongma area. The  $\tau''(1)$  values for Cu (0.378) and Bi (0.426) in Gongma area are the minimum (Table 2), which may represent a new insight into evaluation of ore-forming potential. The coherence of the multifractal parameters indicates that the Gongma area may be the most favorable area for Cu and Bi mineralization and the most prospective area for Cu and Bi.

**Table 2** Multifractal parameters of geochemical data per element analyzed in stream sediments from four subareas in the Bange region, Tibet

| Location          | Parameter        | Au    | Ag     | As    | Cu     | Mo     | Pb    | Zn     | W     | Sn     | Bi    | Sb     | Hg    |
|-------------------|------------------|-------|--------|-------|--------|--------|-------|--------|-------|--------|-------|--------|-------|
| Duoba area        | $\Delta\alpha$   | 1.708 | 0.860  | 0.702 | 0.992  | 0.321  | 0.824 | 0.584  | 0.969 | 1.59   | 1.081 | 0.685  | 0.887 |
|                   | $\Delta\alpha_R$ | 0.585 | 0.191  | 0.254 | 0.625  | 0.161  | 0.072 | 0.433  | 0.260 | 0.485  | 0.265 | 0.278  | 0.096 |
|                   | $\Delta\alpha_L$ | 1.122 | 0.669  | 0.448 | 0.367  | 0.160  | 0.752 | 0.151  | 0.710 | 1.105  | 0.816 | 0.408  | 0.791 |
|                   | $R$              | 0.314 | 0.556  | 0.277 | -0.260 | -0.002 | 0.825 | -0.482 | 0.464 | 0.390  | 0.509 | 0.190  | 0.783 |
|                   | $\tau''(1)$      | 0.950 | 0.998  | 0.988 | 1.003  | 1.009  | 1.004 | 1.014  | 0.969 | 0.961  | 0.982 | 0.994  | 0.997 |
| Gongma area       | $\Delta\alpha$   | 0.770 | 1.819  | 0.695 | 2.231  | 1.544  | 1.378 | 1.667  | 1.375 | 1.612  | 2.251 | 0.869  | 0.745 |
|                   | $\Delta\alpha_R$ | 0.310 | 0.169  | 0.237 | 0.262  | 0.240  | 0.119 | 0.574  | 0.270 | 0.429  | 0.208 | 0.203  | 0.087 |
|                   | $\Delta\alpha_L$ | 0.460 | 1.642  | 0.458 | 1.943  | 1.304  | 1.259 | 1.093  | 1.105 | 1.183  | 2.035 | 0.666  | 0.658 |
|                   | $R$              | 0.195 | 0.814  | 0.318 | 0.762  | 0.689  | 0.827 | 0.311  | 0.608 | 0.468  | 0.814 | 0.533  | 0.767 |
|                   | $\tau''(1)$      | 0.980 | 0.713  | 0.982 | 0.378  | 0.898  | 0.863 | 0.899  | 0.898 | 0.889  | 0.426 | 0.981  | 0.986 |
| Jiurucuo area     | $\Delta\alpha$   | 1.64  | 0.157  | 0.683 | 0.776  | 0.550  | 0.163 | 0.588  | 0.552 | 0.319  | 1.309 | 0.478  | 0.441 |
|                   | $\Delta\alpha_R$ | 0.504 | 0.093  | 0.230 | 0.623  | 0.129  | 0.060 | 0.235  | 0.252 | 0.184  | 0.223 | 0.112  | 0.090 |
|                   | $\Delta\alpha_L$ | 1.135 | 0.064  | 0.453 | 0.153  | 0.421  | 0.104 | 0.353  | 0.301 | 0.135  | 1.085 | 0.366  | 0.351 |
|                   | $R$              | 0.384 | -0.187 | 0.328 | -0.606 | 0.530  | 0.271 | 0.201  | 0.089 | -0.154 | 0.659 | 0.533  | 0.590 |
|                   | $\tau''(1)$      | 0.992 | 1.031  | 1.023 | 1.024  | 1.013  | 1.029 | 1.019  | 1.021 | 1.023  | 0.985 | 1.022  | 1.028 |
| Bange County area | $\Delta\alpha$   | 1.939 | 0.324  | 0.65  | 0.666  | 0.313  | 0.104 | 0.262  | 0.931 | 1.276  | 0.72  | 0.609  | 1.169 |
|                   | $\Delta\alpha_R$ | 0.440 | 0.139  | 0.233 | 0.166  | 0.139  | 0.051 | 0.144  | 0.031 | 0.192  | 0.161 | 0.319  | 0.119 |
|                   | $\Delta\alpha_L$ | 1.427 | 0.185  | 0.417 | 0.500  | 0.173  | 0.053 | 0.117  | 0.900 | 1.085  | 0.559 | 0.290  | 1.051 |
|                   | $R$              | 0.528 | 0.143  | 0.283 | 0.501  | 0.108  | 0.027 | -0.103 | 0.933 | 0.699  | 0.554 | -0.048 | 0.797 |
|                   | $\tau''(1)$      | 0.831 | 1.070  | 1.058 | 1.061  | 1.059  | 1.070 | 1.062  | 0.999 | 0.983  | 1.052 | 1.070  | 1.043 |

Note:  $\Delta\alpha$ . The width of the multifractal spectrum curve;  $\Delta\alpha_R$ . the width of the right part of the multifractal spectrum curve;  $\Delta\alpha_L$ . the width of the left part of the multifractal spectrum curve;  $R$ . the asymmetry index of the multifractal spectrum curve;  $\tau''(1)$ . the multifractality when  $q=1$ .

### 3.2 Petrochemical Analysis of Rock Chips

The mineral exploration in the Bange region was conducted during 2008–2010, and eight Cu-Fe occurrences (Fig. 1a) and some mineralization clues were discovered. It was shown that the NW-tending mineralized zone was mainly controlled by the intrusion of the Late Cretaceous granitoid pluton (monzonitic granite), and the ore-bodies occurred in the contact zones between the pluton and limestones of the Lower Cretaceous Langshan Formation. The main ore minerals are chalcop-

pyrite and magnetite, and the secondary minerals are malachite and azurite.

A total of 37 Cu-Fe rock chip samples were collected from five locations including Biangari (BGR), Duoria (DRA), Longga (LG), Quru (QR) and Gangguo (GG) (Fig. 1a), and the geochemical data for Cu, Pb, Zn, and Ag are shown in Table 3. Petrochemical analysis shows that the ranges of concentrations of Cu, Pb, Zn and Ag in rock chip samples are 1.11%–19.40%, 0.005%–2.18%, 0.05%–9.77%, 8.46 ppm–426.00 ppm, respec-



tively. According to the specifications for Cu, Pb, Zn, Ag, Ni and Mo mineral exploration in China (Ministry of Land and Resources of China, 2002), the Cu contents of 37 rock (ore) chip samples all exceed the cutoff industrial grade (Cu 0.5%) while some of the Pb, Zn and Ag contents are over 0.2%, 0.4% and 1 ppm, respectively, which are the minimum grades for associated components in a copper deposit.

Bismuth is a rare element in the nature, and its average

contents in the ultrabasic rock, the basic rock, the intermediate rock, the acid rock and the crust are 1 ppm, 7 ppm, 10 ppm, 10 ppm and 0.004 ppm, respectively (Liu and Cao, 1987). Nineteen skarn type rock chip samples were collected from three localities named Chalangla (CLL), Xueru (XR) and Gengnai (GN) in the Gongma area and the Bi contents in the rock chips were detected (Zhao et al., 2010) (Table 3). The concentrations of Bi range from 26.9 ppm to 1 317 ppm, with an average

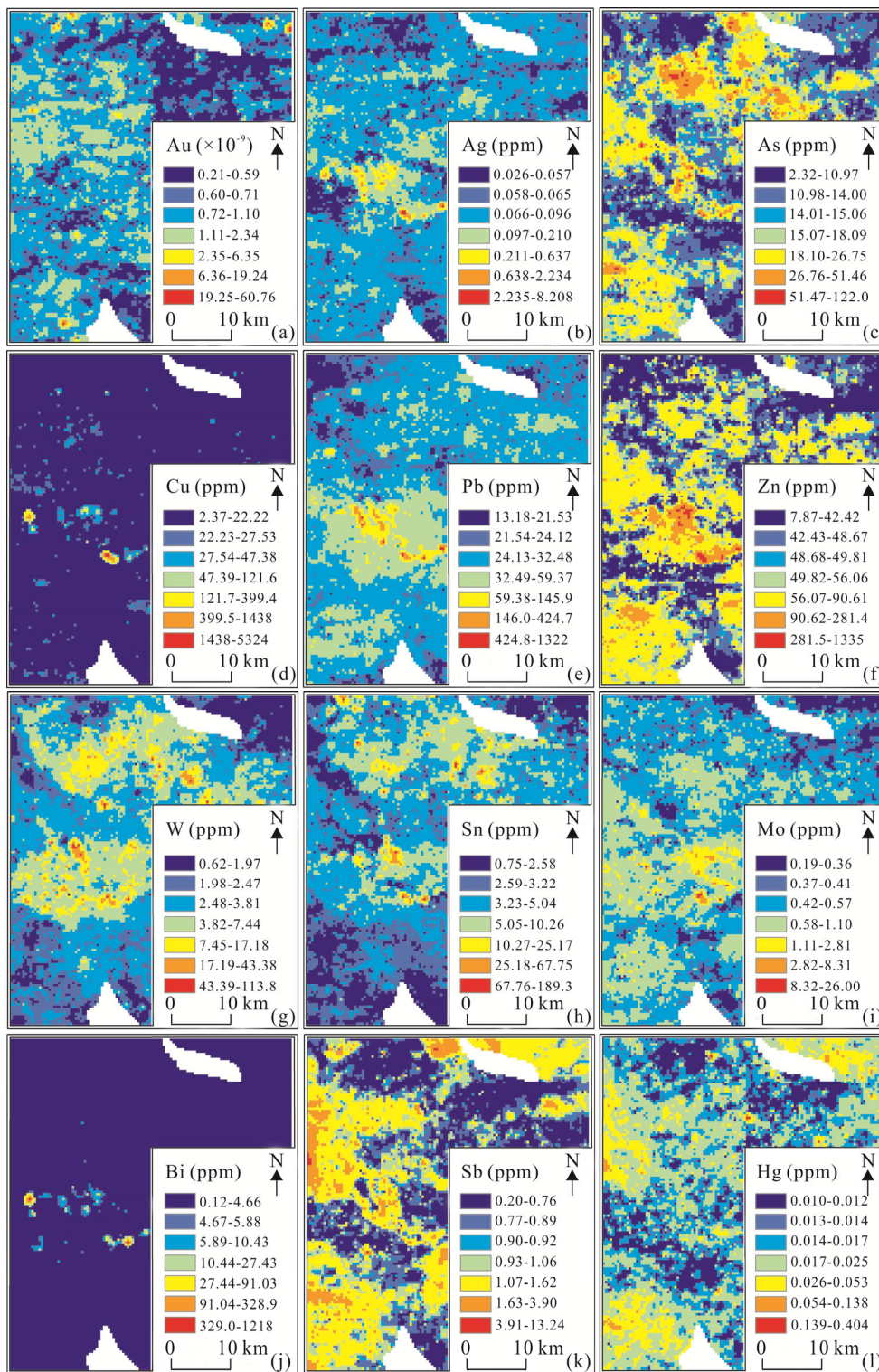


Figure 3. Geochemical maps of 12 elements in stream sediments of the Bange region, Tibet.

**Table 3** Contents of Cu, Pb, Zn, Ag and Bi in rock (ore) chip from the Gongma area in the Bange region, Tibet

| Location          | Sample No.   | Cu (%) | Pb (%) | Zn (%) | Ag ( $\mu\text{g/g}$ ) | Location   | Sample No. | Bi ( $\mu\text{g/g}$ ) |
|-------------------|--------------|--------|--------|--------|------------------------|--|------------|------------------------|
| Biangari<br>(BGR) | 1-01         | 2.55   | 2.18   | 1.67   | <0.001                 | Chalangla<br>(CLL)   | CLL-4      | 34                     |
|                   | 1-02         | 4.20   | 0.17   | 0.45   | <0.001                 |  | CLL-4      | 218                    |
|                   | 2-01         | 3.43   | 0.10   | 0.27   | <0.001                 |  | CLL-4      | 26.9                   |
|                   | 2-02         | 3.07   | 0.14   | 3.08   | 33.80                  | Xueru<br>(XR)  | XR-3       | 32.8                   |
|                   | 2-03         | 2.64   | 0.17   | 5.52   | 30.10                  |  | XR-4       | 64.2                   |
|                   | 2-04         | 19.40  | 0.10   | 1.42   | 350.00                 |  | XR-5       | 793                    |
|                   | 2-05         | 17.00  | 0.07   | 1.40   | 295.00                 |  | XR-7       | 723                    |
|                   | 2-06         | 4.25   | 0.03   | 0.17   | 18.30                  |  | XR-8       | 141                    |
| 2-07              | 8.61         | 1.39   | 5.14   | 112.00 | Gengnai<br>(GN)        | GN-9   | 304        |                        |
| Duoria<br>(DRA)   | 3-01         | 3.33   | 0.01   | 0.26   |                        | 11.50  | GN-16      | 67.7                   |
|                   | 3-02         | 15.74  | 0.03   | 1.74   |                        | 19.80  | GN-17      | 31.8                   |
|                   | 3-03         | 10.74  | 0.04   | 0.73   |                        | 10.10  | GN-34      | 34.7                   |
|                   | 3-04         | 10.85  | 0.02   | 0.76   |                        | 21.70  | GN-35      | 1317                   |
|                   | 3-05         | 8.63   | 0.06   | 1.04   |                        | 8.46   | GN-37      | 466                    |
|                   | 3-06         | 5.76   | 0.03   | 1.07   |                        | 8.47   | GN-38      | 125                    |
|                   | 3-07         | 7.73   | 0.15   | 1.28   |                        | 33.30  | GN-39      | 465                    |
|                   | 3-08         | 10.26  | 0.06   | 0.55   |                        | 12.20  | GN-40      | 135                    |
| Longga<br>(LG)    | 4-01         | 1.11   | 0.08   | 0.23   |                        | 19.20  | GN-41      | 196                    |
|                   | 4-02         | 2.44   | 0.01   | 0.42   | 11.30                  | GN-42  | 150        |                        |
|                   | 4-03         | 2.39   | 0.02   | 0.35   | 10.90                  | Note: The Bi contents data were cited from Zhao et al. (2010). |            |                        |
|                   | 5-01         | 1.40   | 0.02   | 0.20   | 23.80                  |  |            |                        |
|                   | 5-02         | 1.19   | 0.01   | 0.25   | 16.20                  |  |            |                        |
|                   | 5-03         | 2.16   | 0.06   | 0.11   | 13.90                  |  |            |                        |
|                   | 5-04         | 1.75   | 0.22   | 0.33   | 57.80                  |  |            |                        |
|                   | Quru<br>(QR) | 6-01   | 1.86   | 0.11   | 0.05                   |  |            | 179.00                 |
| 6-02              |              | 2.17   | 0.20   | 0.22   | 33.60                  |  |            |                        |
| 6-03              |              | 1.28   | 0.18   | 0.26   | <0.001                 |  |            |                        |
| 6-04              |              | 1.26   | 0.08   | 2.40   | <0.001                 |  |            |                        |
| 7-01              |              | 1.34   | 0.04   | 1.10   | <0.001                 |  |            |                        |
| 7-02              |              | 1.22   | <0.005 | <0.005 | <0.001                 |  |            |                        |
| 7-03              |              | 1.19   | <0.005 | <0.005 | 19.40                  |  |            |                        |
| 7-04              |              | 1.23   | <0.005 | <0.005 | <0.01                  |  |            |                        |
| Gangguo<br>(GG)   | 8-01         | 2.39   | 1.12   | 9.77   | 426.00                 |  |            |                        |
|                   | 8-02         | 1.58   | <0.005 | <0.005 | <0.001                 |  |            |                        |
|                   | 8-03         | 1.64   | <0.005 | <0.005 | <0.001                 |  |            |                        |
|                   | 8-04         | 1.85   | 1.64   | 8.88   | 344.00                 |  |            |                        |
|                   | 8-05         | 4.04   | 0.01   | 0.07   | 37.40                  |  |            |                        |

concentration of 280.3 ppm, which are significantly higher than that of different types rocks both in the earth and in different metallogenic belts in the Tibetan Plateau (Zhao et al., 2010). Moreover, the Bi contents of two samples (GN-37 and GN-39) are close to the cutoff industrial grade 500 ppm, three samples (XR-5, XR-7 and GN-35) exceed the cutoff industrial grade and one sample (GN-35) reaches the industrial grade 1 000 ppm (He et al., 2004).

These petrochemical results show that Cu and Bi are extremely enriched in the Gongma area, which are in agreement with the results of the multifractal analysis. The results imply

that there is a good ore-forming potential and prospectivity for Cu and Bi in the Gongma area. It can be concluded that all the results obtained by the method of moments are consistent with petrochemical analysis and field observation (Fig. 4), which show that Cu-Bi polymetallic mineralization of skarn type is present in the Gongma area (Gao, et al., 2011a; Song, 2011).

#### 4 CONCLUSIONS

Multifractal techniques have been used to characterize spatial structures of geochemical fields for mineral exploration. In this work, a total of 7 270 stream sediment samples were



collected from four subareas in northern Tibet, Southwest China. Concentrations of twelve elements were measured per sample. The method of moments was used and several multifractal parameters were obtained to characterize the multifractal properties of the distribution patterns of element concentrations. The work obtained the following conclusion.

1. The multifractality for Cu and Bi in the Gongma area are much stronger than in the other three subareas. The asymmetry index of multifractal spectra and variance of Cu and Bi

are the highest in the Gongma area compared to the other three areas, implying that the distribution pattern of Cu and Bi in this area are the most heterogeneous. The Gongma area is the most favorable area for prospecting Cu and Bi.

2. The coherence between the results obtained by the method of moments and the petrochemical analysis shows that Cu-Bi polymetallic mineralization of skarn type is present in the Gongma area. Multifractal analysis may provide more new avenues for geochemical exploration.

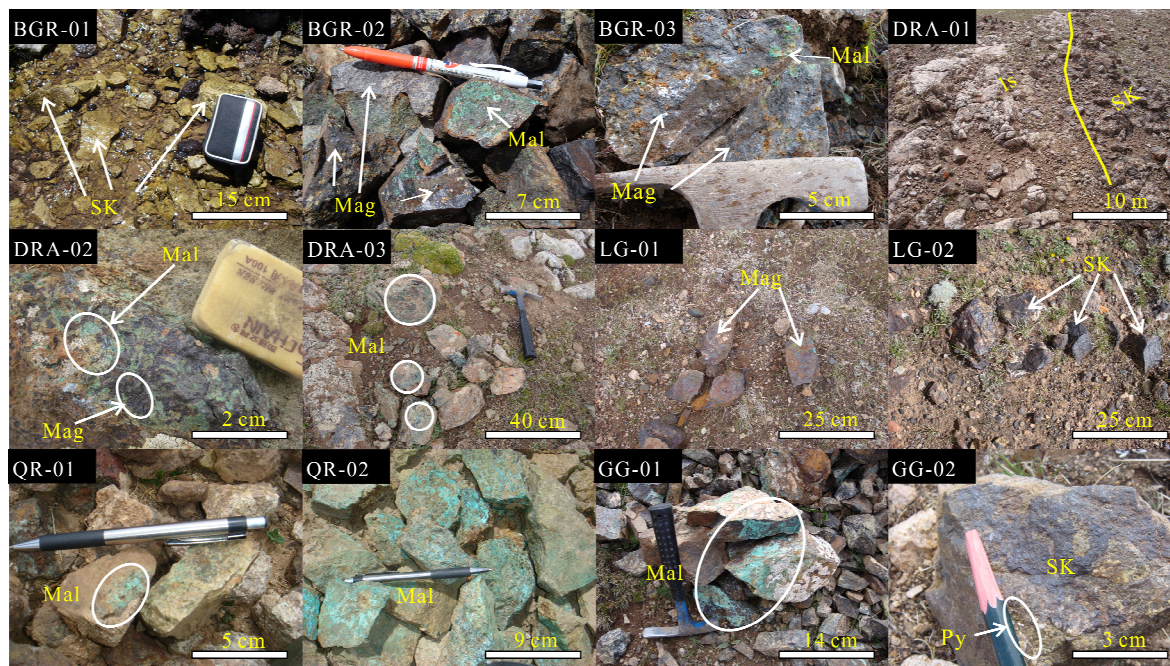


**Figure 4.** Photographs of skarns and Cu-Fe ores in the Bange region, Tibet (Mal. malachite; Mag. magnetite; Py. pyrite; SK. skarn; ls. limestone).

#### ACKNOWLEDGMENTS

This study was financially supported by the Special Project on Mineral Exploration and Assessment in Tibetan Plateau (No. 1212010818038), the Program for Changjiang Scholars and Innovative Research Team in University of Ministry of Education of China (No. IRT1083), and the National Natural Science Foundation of China (No. 41272362). The authors thank Dr. Qiuming Cheng (GPMR, China University of Geosciences) and Dr. John Carranza (James Cook University) for their constructive comments and suggestions. We gratefully acknowledge reviewers for constructive reviews, and editors for kind help on the early draft.

#### REFERENCES CITED

- Agterberg, F. P., 2001. Multifractal Simulation of Geochemical Map Patterns. *Journal of China University of Geosciences*, 12(1): 31–39. doi:10.1007/978-1-4615-1359-9\_17
- Carlson, C. A., 1991. Spatial Distribution of Ore Deposits. *Geology*, 19(2): 111–114. doi:10.1130/0091-7613(1991)019<0111:SDOOD>2.3.CO
- Carranza, E. J. M., 2009. Controls on Mineral Deposit Occurrence Inferred from Analysis of Their Spatial Pattern and Spatial Association with Geological Features. *Ore Geology Reviews*, 35(3–4): 383–400. doi:10.1016/j.oregeorev.2009.01.001
- Cheng, Q. M., 1995. The Perimeter-Area Fractal Model and Its Application to Geology. *Mathematical Geology*, 27(1): 69–82. doi:10.1007/BF02083568
- Cheng, Q. M., 1999a. Spatial and Scaling Modeling for Geochemical Anomaly Separation. *Journal of Geochemical Exploration*, 65(3): 175–194. doi:10.1016/S0375-6742(99)00028-X
- Cheng, Q. M., 1999b. Multifractality and Spatial Statistics. *Computers and Geosciences*, 25(9): 949–961. doi:10.1016/S0098-3004(99)00060-6
- Cheng, Q. M., 2000a. Multifractal Theory and Geochemical Element Distribution Pattern. *Earth Science—Journal of China University of Geosciences*, 25(3): 311–318 (in Chinese with English Abstract)
- Cheng, Q. M., 2000b. GeoData Analysis System (GeoDAS) for Mineral Exploration: User's Guide and Exercise Manual. Material for the Training Workshop on GeoDAS Held at York University, Toronto
- Cheng, Q. M., Agterberg, F. P., 1995. Multifractal Modeling and Spatial Point Processes. *Mathematical Geology*, 27(7): 831–845. doi:10.1007/BF02087098
- Cheng, Q. M., Agterberg, F. P., 1996. Multifractal Modeling and Spatial Statistics. *Mathematical Geology*, 28(1): 1–16.

- doi:10.1007/BF02273520
- Cheng, Q. M., Agterberg, F. P., Ballantyne, S. B., 1994. The Separation of Geochemical Anomalies from Background by Fractal Methods. *Journal of Geochemical Exploration*, 51(2): 109–130. doi:10.1016/0375-6742(94)90013-2
- Cheng, Q. M., Agterberg, F. P., Bonham-Carter, G. F., 1996. A Spatial Analysis Method for Geochemical Anomaly Separation. *Journal of Geochemical Exploration*, 56(3): 183–195. doi:10.1016/S0375-6742(96)00035-0
- Cheng, Q. M., Bonham-Carter, G. F., Hall, G. E. M., et al., 1997. Statistical Study of Trace Elements in the Soluble Organic and Amorphous Fe-Mn Phases of Surficial Sediments, Sudbury Basin. 1. Multivariate and Spatial Analysis. *Journal of Geochemical Exploration*, 59(1): 27–46. doi:10.1016/S0375-6742(96)00046-5
- Evertsz, C. J. G., Mandelbrot, B. B., 1992. Multifractal Measures(Appendix B). In: Peitgen, H. O., Jurgens, H., Saupe, D., eds., *Chaos and Fractals*. Springer-Verlag, New York
- Feder, J., 1988. *Fractals*. Plenum Press, New York
- Gao, S. B., Zheng, Y. Y., Wang, J. S., et al., 2011a. The Geochronology and Geochemistry of Intrusive Rocks in Bange Area: Constraints on the Evolution Time of the Bangong Lake-Nujiang Ocean Basin. *Acta Petrologica Sinica*, 27(7): 1973–1982 (in Chinese with English Abstract)
- Gao, S. B., Zheng, Y. Y., Xie, M. C., et al., 2011b. Geodynamic Setting and Mineralizational Implication of the Xueru Intrusion in Ban'ge, Tibet. *Earth Science—Journal of China University of Geosciences*, 36(4): 729–739 (in Chinese with English Abstract)
- Grunsky, E. C., Agterberg, F. P., 1988. Spatial and Multivariate Analysis of Geochemical Data from Metavolcanic Rocks in the Ben Nevis Area, Ontario. *Mathematical Geology*, 20(7): 825–861. doi:10.1007/BF00890195
- Gumiel, P., Sanderson, D. J., Arias, M., et al., 2010. Analysis of the Fractal Clustering of Ore Deposits in the Spanish Iberian Pyrite Belt. *Ore Geology Reviews*, 38(4): 307–318. doi:10.1016/j.oregeorev.2010.08.001
- He, Z. H., Li, S. Q., Hu, Z. K., 2004. Discussion on Industrial Index of Bismuth Deposit. *Geology and Mineral Resources of South China*, 2: 32–34 (in Chinese with English Abstract)
- Halsey, T. C., Jensen, M. H., Kadanoff, L. P., et al., 1986. Fractal Measures and Their Singularities—The Characterization of Strange Sets. *Physical Review A*, 33(2): 1141–1151. doi:10.1103/PhysRevA.33.1141
- Hou, Z. Q., Yang, Z. M., Qu, X. M., et al., 2009. The Miocene Gangdese Porphyry Copper Belt Generated during Post-Collisional Extension in the Tibetan Orogen. *Ore Geology Review*, 36(3): 25–51. doi:10.1016/j.oregeorev.2008.09.006
- Li, C. J., Xu, Y. L., Jiang, X. L., 1994. The Fractal Model of Mineral Deposits. *Geology of Zhejiang*, 10(2): 25–32 (in Chinese with English Abstract)
- Li, G. M., Pan, G. T., Wang, G. M., et al., 2004. Evaluation and Prospecting Value of Mineral Resources in Gangdise Metallogenic Belt, Tibet, China. *Journal of Chengdu University of Technology (Science & Technology Edition)*, 31(1): 22–27 (in Chinese with English Abstract)
- Li, G. M., She, H. Q., Zhang, L., et al., 2009. Based on Mineral Resource Assessment System (MRAS) for the Metallogenic Prognosis in Gangdese Metallogenic Belt, Tibet. *Geology and Exploration*, 45(6): 645–654 (in Chinese with English Abstract)
- Liu, Y. J., Cao, L. M., 1987. *An Introduction on Elements Geochemistry*. Geological Publishing House, Beijing (in Chinese)
- Mandelbrot, B. B., 1983. *The Fractal Geometry of Nature*. W. H. Freeman, New York
- Ministry of Land and Resources of China, 2002. Specifications for Copper, Lead, Zinc, Silver, Nickel and Molybdenum Mineral Exploration. Geology and Mineral Resource Industry Standard of the PRC (DZ/T 0214-2002), Beijing (in Chinese)
- Pan, G. T., Mo, X. X., Hou, Z. Q., et al., 2006. Spatial-Temporal Framework of the Gangdese Orogenic Belt and Its Evolution. *Acta Petrologica Sinica*, 22(3): 521–533 (in Chinese with English Abstract)
- Qu, X. M., Hou, Z. Q., Huang, W., 2001. Is Gangdese Porphyry Copper Belt the Second “Yulong” Copper Belt? *Mineral Deposits*, 20(4): 355–366 (in Chinese with English Abstract)
- Raines, G. L., 2008. Are Fractal Dimensions of the Spatial Distribution of Mineral Deposits Meaningful? *Natural Resources Research*, 17(2): 87–97. doi:10.1007/s11053-008-9067-8
- Rui, Z. Y., Hou, Z. Q., Qu, X. M., et al., 2003. Metallogenic Epoch of Gangdese Porphyry Copper Belt and Uplift of Qinghai-Tibet Plateau. *Mineral Deposits*, 22(3): 217–225 (in Chinese with English Abstract)
- Rui, Z. Y., Li, G. M., Zhang, L. S., et al., 2006. Metallic Ore Deposits on the Qinghai-Tibet Plateau. *Geology in China*, 33(2): 363–373 (in Chinese with English Abstract)
- Sanderson, D. J., Roberts, S., Gumiel, P., 1994. A Fractal Relationship between Vein Thickness and Gold Grade in Drill Core from La Codosera, Spain. *Economic Geology*, 89(1): 168–173. doi:10.2113/gsecongeo.89.1.168
- She, H. Q., Li, G. M., Dong, Y. J., et al., 2009. Regional Metallogenic Prognosis and Mineral Reserves Estimation for Porphyry Copper Deposits in Gangdese Polymetallic Ore Belt, Tibet. *Mineral Deposits*, 28(6): 803–814 (in Chinese with English Abstract)
- Shi, J. F., Wang, C. N., 1998. Fractal Analysis of Gold Deposits in China: Implication for Giant Deposit Exploration. *Earth Science—Journal of China University of Geosciences*, 23(6): 616–618 (in Chinese with English Abstract)
- Sinclair, A. J., 1991. A Fundamental Approach to Threshold Estimation in Exploration Geochemistry: Probability Plots Revisited. *Journal of Geochemical Exploration*, 41(1–2): 1–22. doi:10.1016/0375-6742(91)90071-2
- Song, L., 2011. The Research About Minerogenetic Series in the Middle of Bangonghu-Nujiang Metallogenic Belt, Tibet: [Dissertation]. China University of Geosciences, Beijing (in Chinese with English Abstract)
- Stanley, C. R., 1988. Comparison of Data Classification Pro-

- cedures in Applied Geochemistry Using Monte Carlo Simulation: [Dissertation]. University of British Columbia, Vancouver
- Stanley, C. R., Sinclair, A. J., 1989. Comparison of Probability Plots and Gap Statistics in the Selection of Threshold for Exploration Geochemistry Data. *Journal of Geochemical Exploration*, 32(1–3): 355–357. doi:10.1016/0375-6742(89)90076-9
- Turcotte, D. L., 1997. *Fractals and Chaos in Geology and Geophysics*, 2nd Edition. Cambridge University Press, Cambridge
- Turcotte, D. L., 2002. Fractals in Petrology. *Lithos*, 65(3–4): 261–271. doi:10.1016/S0024-4937(02)00194-9
- Wang, Q. H., Wang, B. S., Li, J. G., et al., 2002. Basic Features and Ore Prospect Evaluation of the Gangdise Island Arc, Tibet, and Its Copper Polymetallic Ore Belt. *Geological Bulletin of China*, 21(1): 35–45 (in Chinese with English Abstract)
- Wang, Z. J., Cheng, Q. M., Cao, L., et al., 2006. Fractal Modeling of the Microstructure Property of Quartz Mylonite during Deformation Process. *Mathematical Geology*, 39(1): 53–68. doi:10.1007/s11004-006-9065-5
- Wang, Z. J., Cheng, Q. M., Xu, D. Y., et al., 2008. Fractal Modeling of Sphalerite Banding in Jinding Pb-Zn Deposit, Yunnan, Southwestern China. *Journal of China University of Geosciences*, 19(1): 77–84. doi:10.1016/S1002-0705(08)60027-8
- Xie, S. Y., 2003. *Fractal and Multifractal Properties of Geochemical Fields*: [Dissertation]. China University of Geosciences, Wuhan
- Xie, S. Y., Bao, Z. Y., 2003a. Multifractal and Geochemical Element Distribution Patterns. *Geology-Geochemistry*, 31(3): 97–102 (in Chinese with English Abstract)
- Xie, S. Y., Bao, Z. Y., 2003b. The Method of Moments and Its Application to the Study of Mineralization in Shaoguan District, North Guangdong, China. *Journal of Jilin University (Earth Science Edition)*, 33(4): 443–448 (in Chinese with English Abstract)
- Xie, S. Y., Bao, Z. Y., 2004a. Fractal and Multifractal Properties of Geochemical Fields. *Mathematical Geology*, 36(7): 847–864. doi:10.1023/B:MATG.0000041182.70233.47
- Xie, S. Y., Bao, Z. Y., 2004b. Application of Multifractal to Ore-Forming Potential Evaluation. *Journal of Chengdu University of Technology (Science & Technology Edition)*, 31(1): 28–33 (in Chinese with English Abstract)
- Xie, S. Y., Cheng, Q. M., Chen, G., et al., 2007. Application of Local Singularity in Prospecting Potential Oil/Gas Targets. *Nonlinear Processes in Geophysics*, 14(3): 285–292. doi:10.5194/npg-14-285-2007
- Xie, S. Y., Cheng, Q. M., Ke, X. Z., et al., 2008. Identification of Geochemical Anomaly by Multifractal Analysis. *Journal of China University of Geosciences*, 19(4): 334–342. doi:10.1016/S1002-0705(08)60066-7
- Xie, S. Y., Cheng, Q. M., Xing, X. T., et al., 2010. Geochemical Multifractal Distribution Patterns in Sediments from Ordered Streams. *Geoderma*, 160(1): 36–46. doi:10.1016/j.geoderma.2010.01.009
- Xie, X. J., Yin, B. C., 1993. Geochemical Patterns from Local to Global. *Journal of Geochemical Exploration*, 47(1–3): 109–129. doi:10.1016/0375-6742(93)90061-P
- Zhang, J. C., Wang, X. W., Lei, C. Y., et al., 2011. Genesis of Late Yanshanian Granites and the Ore-Search Prospect in the Duoba-Bange Area, Gangdise Belt, Tibet, China. *Journal of Chengdu University of Technology (Science and Technology Edition)*, 38(6): 671–677 (in Chinese with English Abstract)
- Zhao, Y. Y., Liu, Y., Wang, R. J., et al., 2010. The Discovery of the Bismuth Mineralization Belt in the Bangong Co-Nujiang Metallogenic Belt of Tibet and Its Adjacent Areas and Its Geological Significance. *Acta Geoscientica Sinica*, 31(2): 183–193 (in Chinese with English Abstract)
- Zheng, Y. Y., Wang, B. S., Fan, Z. H., et al., 2002. Analysis of Tectonic Evolution in the Eastern Section of the Gangdise Mountains, Tibet and the Metallogenic Potentialities of Copper Gold Polymetal. *Geological Science and Technology Information*, 21(2): 55–60 (in Chinese with English Abstract)
- Zheng, Y. Y., Xue, Y. X., Gao, S. B., 2003. Copper-Polymetal Metallogenic Series and Prospecting Perspective of Eastern Section of Gangdise. *Earth Science—Journal of China University of Geosciences*, 14(4): 349–355 (in Chinese with English Abstract)
- Zhu, D. C., Pan, G. T., Mo, X. X., et al., 2006. Late Jurassic–Early Cretaceous Geodynamic Setting in Middle-northern Gangdese: New Insights from Volcanic Rocks. *Acta Petrologica Sinica*, 22(3): 534–546 (in Chinese with English Abstract)
- Zuo, R. G., 2011. Identifying Geochemical Anomalies Associated with Cu and Pb-Zn Skarn Mineralization using Principal Component Analysis and Spectrum-Area Fractal Modeling in the Gangdese Belt, Tibet (China). *Journal of Geochemical Exploration*, 111(1–2): 13–22. doi:10.1016/j.gexplo.2011.06.012
- Zuo, R. G., Cheng, Q. M., Agterberg, F. P., et al., 2009. Application of Singularity Mapping Technique to Identification Local Anomalies Using Stream Sediment Geochemical Data: A Case Study from Gangdese, Tibet, Western China. *Journal of Geochemical Exploration*, 101(3): 225–235. doi:10.1016/j.gexplo.2008.08.00